Supplementary Information for

Control of Electrons' Spin Eliminates Hydrogen Peroxide Formation During Water Splitting

Wilbert Mtangi[1], Francesco Tassinari[1], Kiran Vankayala [1], Andreas Vargas Jentzsch[2], Beatrice Adelizzi[2], Anja R.A. Palmans[2], Claudio Fontanesi[3], E.W. Meijer*[2], Ron Naaman*[1]

[1]Department of Chemical Physics, Weizmann Institute of Science, Rehovot 76100, Israel;
[2]Institute for Complex Molecular Systems, Eindhoven University of Technology, Eindhoven, the Netherlands;
[3]Department of Engineering, University of Modena and Reggio Emilia, Via Vivarelli 10, 41125 Modena, Italy

This file includes:

Contents

Materials and Methods:

Synthesis of Molecules:

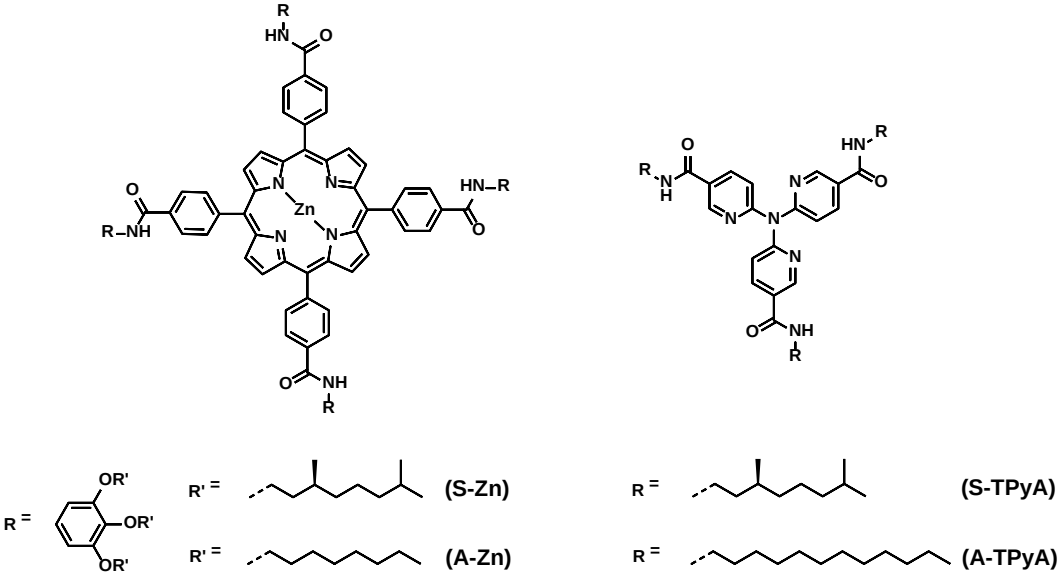

Scheme S1: Molecular structure of chiral and achiral Zn-porphyrins (***S*-Zn** and **A-Zn** respectively) and tri(pyrid-2-yl)amine trisamide (***S*-TPyA** and **A-TPyA**)

Achiral and chiral Zn-porphyrins were synthetized following the procedure reported by Helmich et al.[1,2] Achiral and chiral tri(pyrid-2-yl)amine trisamides were synthesized from the carboxylic acid precursor as follows.[3,4]

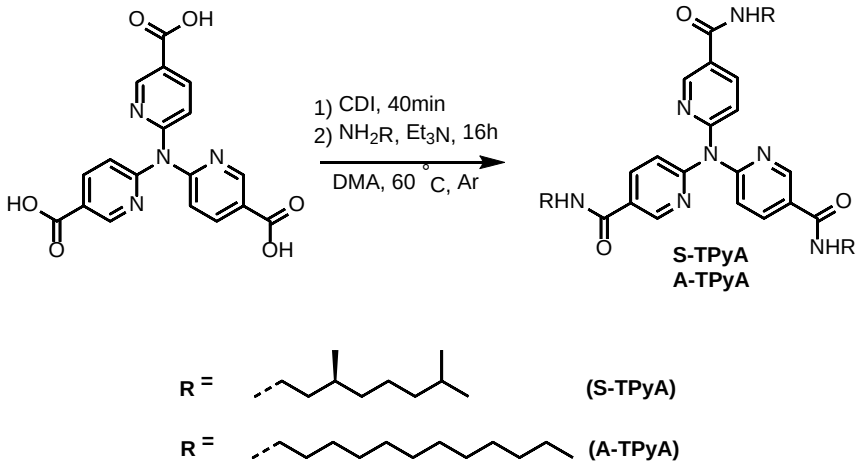

Scheme S2: Amide coupling of TPyA with achiral (**A-TPyA**) and (*S*)-chiral chains (***S*-TPA**)

Preparation of TiO_2 electrodes

TiO_2 nanoparticulate films were deposited on fluorine-doped tin oxide, FTO (surface resistivity of ~7 Ω/sq,) coated glass, purchased from Sigma Aldrich Co., using the electrophoretic deposition (EPD) technique. This technique has been used previously to deposit TiO_2 nanoparticles.[5] A suspension of TiO_2 nanoparticles (NPs) was prepared by dispersing 0.4g TiO_2 NPs (<25nm in diameter and 99.7% trace metals, purchased from Sigma Aldrich Co.) in 40 mL of de-ionized water. Prior to making dispersions, TiO_2 nanoparticle powders were heated at 570 K for 1 h. The mixture was stirred overnight to ensure homogeneity. Prior to nanoparticle deposition, the FTO substrates were boiled in isopropanol for 15 minutes, followed by 15 minutes of boiling in ethanol, and finally rinsed with de-ionized water. After rinsing, the substrates were dried using nitrogen gas and annealed for 15 minutes at T=570 K. EPD was then performed with a Princeton potentiostat using the galvanic pulses mode technique with two pulses (Pulse 1 and Pulse 2). Pulse 1 was set to 0 mA for 200 ms for depolarization. Pulse 2 was varied between 0.50 to 0.95 mA to obtain a maximum potential of 10.0 V. Pulse 2 was applied for 1000 ms in each cycle for polarization, and the number of iterations (pulse 1 followed by pulse 2) was set to 1500. Various cycles were used to prepare films of required thicknesses. The samples were annealed in between cycles at 570 K for 15 minutes in air. During EPD, the suspension was continuously stirred using a magnetic stirrer. After completion of the last cycle, the electrodes were annealed again for 8 h at 570 K.

To confirm the surface coverage of the EPD-deposited TiO_2 NP on FTO, high-resolution scanning electron microscope (SEM) measurements were performed using In-lens-detector imaging with a LEO-Supra 55 VP. The SEM images in Figure S1 show a high surface coverage of the TiO_2 NP on FTO substrates deposited using the EPD technique. An average film thickness of around 5.0 μm was measured, using a Dektak stylus profilometer.

Functionalization of TiO_2 electrodes

TiO_2 electrodes were functionalized with chiral and achiral Zn-porphyrins by drop casting 30μL of the porphyrin solutions on a 1.5 cm^2 area and leaving them overnight to dry under dark and controlled humidity conditions. The porphyrin solutions were made from

porphyrin powders dissolved in methylcyclohexane (MCH) to a concentration of $1.7 \times 10^{-5} M$. Absorbance measurements were conducted on these solutions to confirm the formation of supramolecular structures. The 390 nm absorption peak in Figure S2 confirms the formation of stacks in solution for both the chiral and achiral Zn-porphyrins. Structural characterization of the TiO_2 modified electrodes was performed using SEM. Zn-porphyrins form supramolecular structures with lengths of approximately 1 μm on the TiO_2 substrate surfaces. The functionalization of the TiO_2 electrodes with TPyA molecules was done by dropcasting 150μL of a $2.3 \times 10^{-5} M$ solution on 1.5 cm^2 substrate surfaces and leaving them to dry overnight. The solutions were prepared by dissolving the TPyA molecules in MCH. To ensure the formation of aggregates, the solutions were warmed up to 368 K and cooled down to room temperature at a rate of 1 $Kmin^{-1}$.

Photoelectrochemical measurements

Photoelectrochemical measurements were conducted in a three-electrode cell, with an Ag/AgCl (saturated KCl) electrode as the reference and a Pt wire as the cathode. A 0.1 M Na_2SO_4 (pH = 6.56) aqueous solution was used as the electrolyte. The activity of the photoelectrodes was characterized by measuring the open circuit potential, OCP in the dark and under illumination at zero current. For the measurements on the Zn-porphyrins modified electrodes, a commercial Xe lamp with an intensity of 80 $mWcm^{-2}$ was used. For the measurements on the TPyA modified electrodes, a mercury lamp with an intensity of 110 $mWcm^{-2}$ was used. The electrodes show a huge response to the illumination, confirming their photo-activities (Figure S5). The response of the photoelectrodes was also examined using linear scan voltammetry by switching the light on and off. It's interesting to note that these photoelectrodes have very high sensitivity to illumination (Figure S6).

Mott-Schottky measurements

The electronic properties of the photoelectrodes were characterized using Mott-Schottky measurements (Figure S7). The measurements were performed in the dark, while sweeping potentials from -0.60 to 0.60 V versus the Ag/AgCl reference electrode. An AC voltage with amplitude of 20 mV was superimposed onto the DC voltages in the defined potential window with frequencies ranging from 200 Hz – 200 kHz. 0.1 M Na_2SO_4 was used as the

electrolyte with a Pt wire as the counter electrode. The flat band potential of each modified electrode was determined by fitting the lower linear part of the data to the equation,

$$\frac{1}{C^2} = \frac{2}{\varepsilon\varepsilon_0 q N_D}\left(E - V_{bi} - \frac{kT}{q}\right),$$

where C is the capacitance, N_D is the net doping density of TiO_2 which can be calculated from the gradient, E is the applied potential, and V_{bi} is the flat band potential. The flat band potential was obtained as an intercept to the horizontal axis where $^1/_{C^2} = 0$. The flat band potential was obtained as -0.51 V versus Ag/AgCl for both the chiral and achiral Zn-porphyrins modified electrodes, and as -0.70 V versus Ag/AgCl for both the chiral and achiral TPyA modified electrodes. This indicates that the electronic properties of the TiO_2 are not affected by molecular modification for each class of molecules used in this study.

Conductive AFM measurements

Samples for magnetic conductive probe atomic force microscopy (mCP-AFM) measurements were prepared by drop-casting 5 μL solutions of chiral/achiral Zn-porphyrin aggregates onto freshly cleaved highly oriented pyrolytic graphite (HOPG) substrate and dried under controlled humidity. The AFM images obtained from the drop-casted Zn porphyrins on highly oriented pyrolytic graphite, HOPG substrates are shown in Figure S8. Large area topography scans were recorded in PeakForce TUNA (PF-TUNA) mode prior to I-V spectroscopy measurements. I-V measurements were carried out using Multimode AFM with Nanoscope V controller (Bruker-Nano, Santa Barbara, CA, U.S.A.). I−V spectroscopy measurements were performed by recording voltage ramps at an applied force of 12 nN, with which the tip contacts the surface. For each spectroscopy measurement the tip was retracted and placed in a new position, which prevents the damage to the sample by the tip. A total of around 2 % of the traces were shorts and 5-8 % of the traces show insulating behavior which were not considered for the analysis. Around 50 I-V traces were recorded and averaged for each magnetic field orientation (Magnet UP and DOWN). A magnetic Fe tip (MESP-LC, Bruker) with nominal spring constant 2.8 N/m was used to acquire I-V curves. The tips are magnetized using a permanent magnet.[6,7] The force constant of each probe used was calibrated using the thermal tune procedure of the software.

Hydrogen peroxide quantification

Seven different sets of electrodes were used during this experiment; bare TiO_2, TiO_2 modified with A-Zn (achiral porphyrin), *S*-Zn (chiral porphyrin), A-TPyA (achiral tripyridylamine), *S*-TPyA (chiral tripyridylamide), mercaptopropionic acid, MPA and an oligopeptide, Al7. In this case, MPA and Al7 were chosen so as to comprehend the observations obtained with the supramolecular aggregates.

Electrochemistry in the chronoamperometry mode was performed with a 0.1 M Na_2SO_4 aqueous solution as the electrolyte and an Ag/AgCl (saturated KCl) reference electrode. A potential was chosen and applied to the bare TiO_2 electrode so that hydrogen and oxygen were evolved on the Pt and working electrodes, respectively. Bubbles were observed on both the Pt and TiO_2 electrode during the electrochemical measurements. Chronoamperometry measurements were conducted for 40 minutes. The presence of hydrogen peroxide was verified in a colorimetric test titration experiment of the used electrolyte, with o-tolidine as a redox indicator. For the colorimetric measurements, 0.8 mL of an o-tolidine solution prepared according to the Elmms-Hauser method[8] (purchased from Sigma Aldrich Co.) were added to 4 mL of the electrolyte solution obtained from the electrochemical cell and left to react for 30 minutes. In the presence of H_2O_2 a yellow colour was observed with an absorption peak at around 436 nm from UV-vis absorption spectroscopy. To estimate the concentration of the hydrogen peroxide produced during electrochemical measurements within a specified period of time, a calibration curve was determined using 30% w/w commercial H_2O_2. Figure S14 shows a calibration curve for the concentration of commercial hydrogen peroxide. Results of the calculated concentrations are presented in Table S1. Interesting enough, in the case where chiral molecules were used, no hydrogen peroxide was detected.

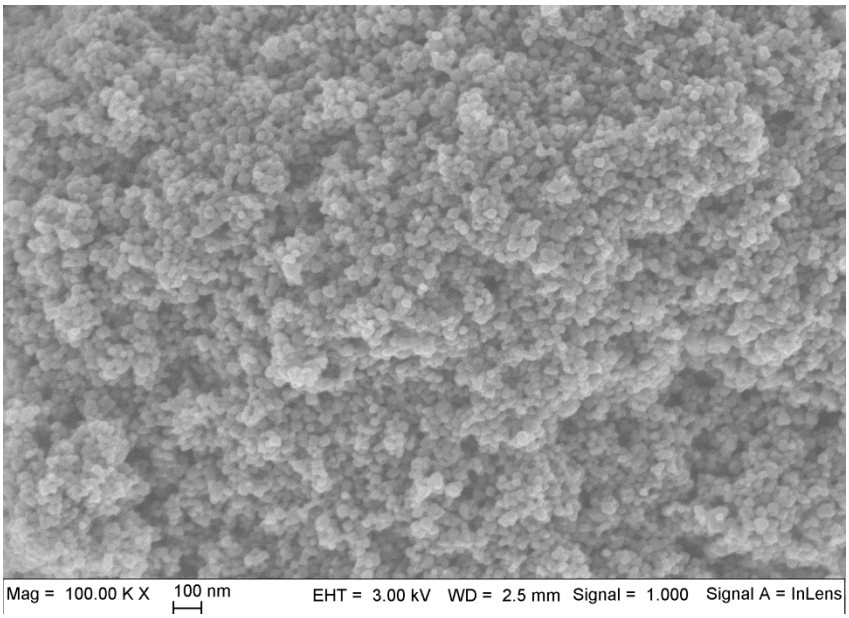

Figure S1: SEM images of EPD TiO_2 nanoparticles on FTO.

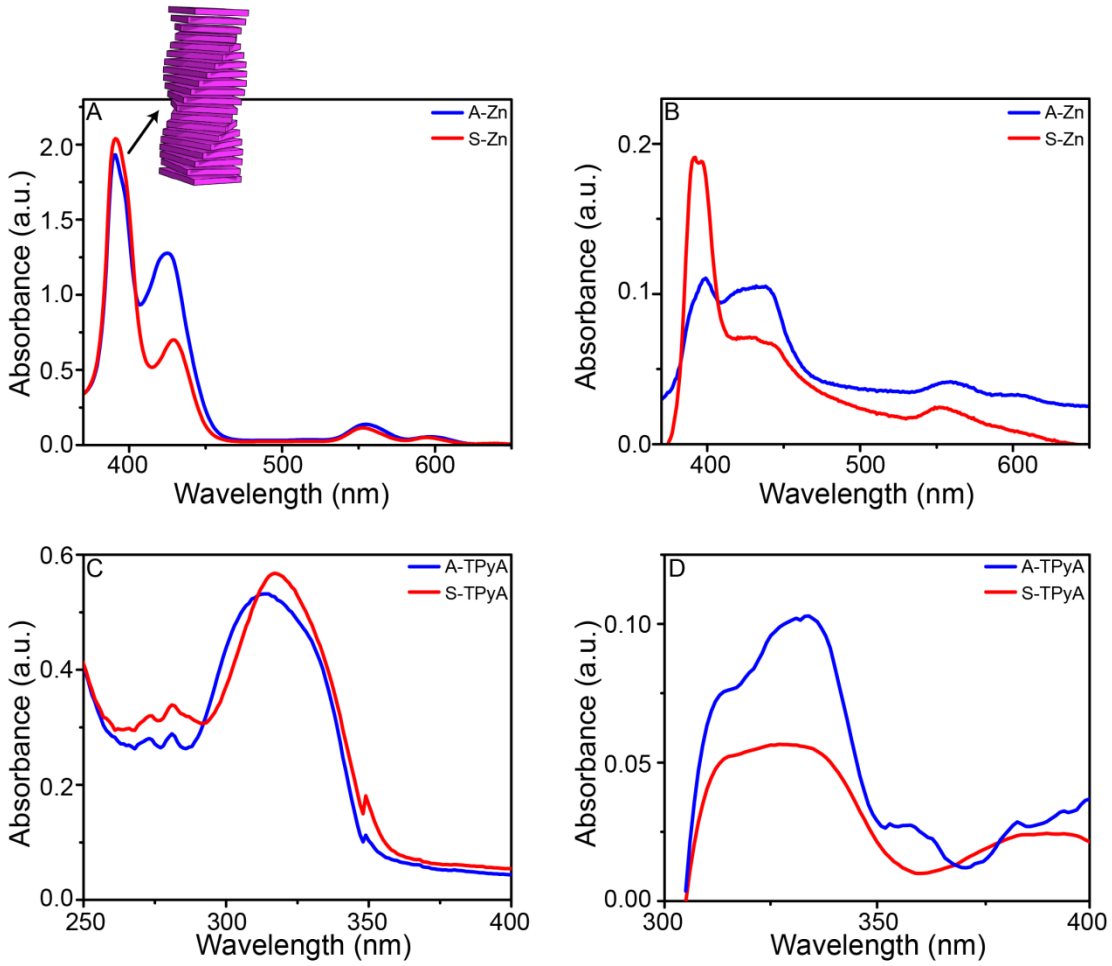

Figure S2: UV-vis spectra, red lines represent chiral analogues, blue lines represent achiral analogues. Zn-porphyrin spectra (**A**) in MCH (c = 1.7 x 10^{-5} M) and on modified TiO_2 substrate (**B**). TPyAs spectra (**C**) in MCH (c = 2.3 x 10^{-5} M) and on modified FTO substrate (**D**).

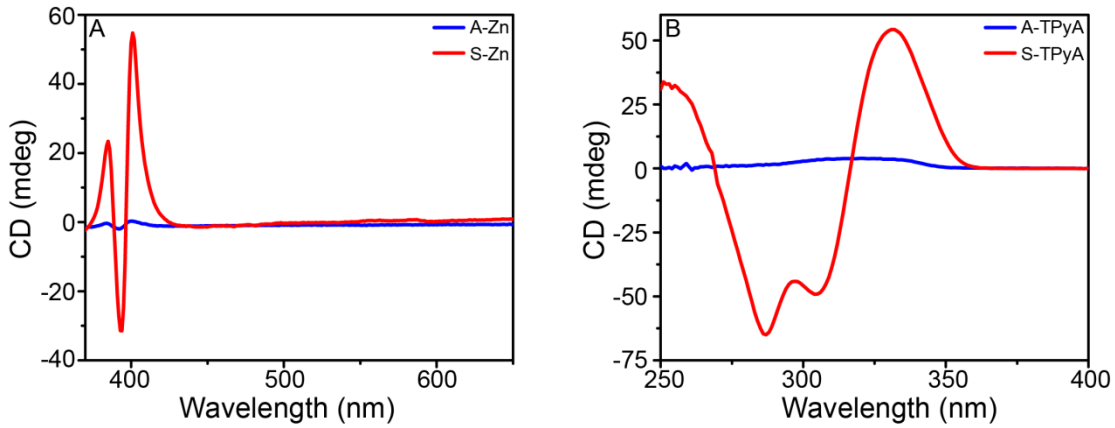

Figure S3: CD spectra of Zn-porphyrin (**A**) (*c* =1.7x10^{-5} M) and (**B**) TPyA (*c* = 2.3 x 10^{-5} M) in MCH.

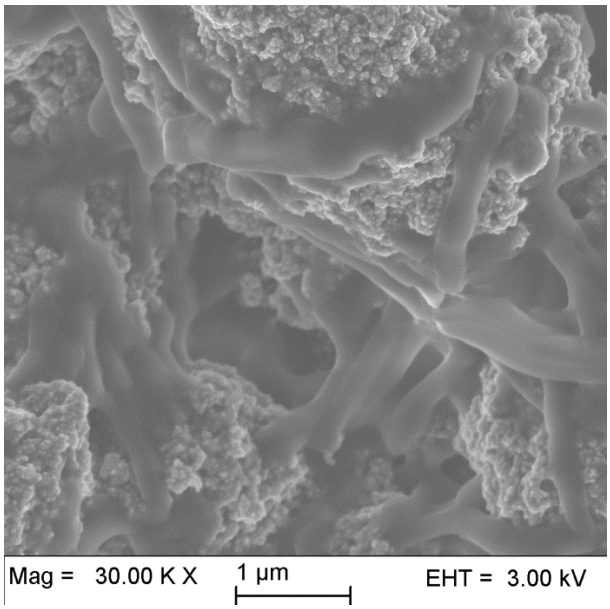

Figure S4: SEM obtained from the Zn-porphyrin molecule modified TiO_2 electrode.

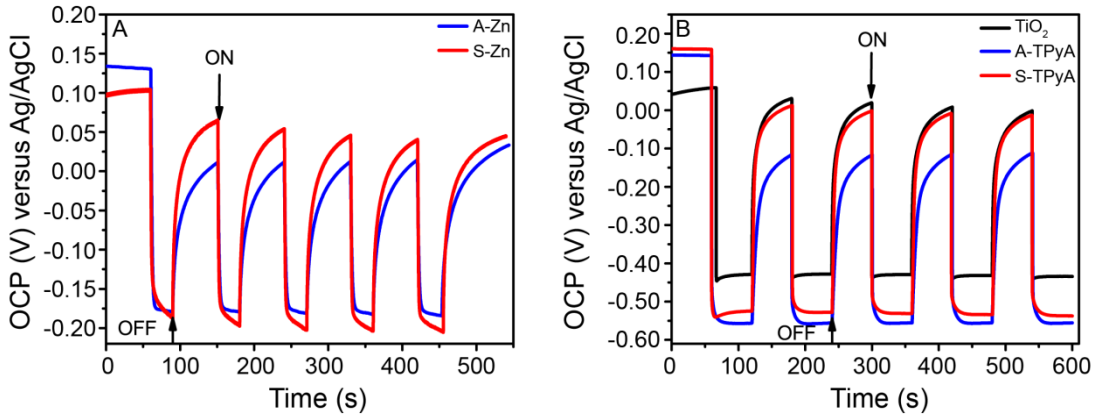

Figure S5: The OCP under dark and illumination as a function of time obtained from the chiral (red) and achiral (blue), (**A**) Zn-porphyrins and (**B**) TPyA modified TiO_2 electrodes. Black line represents the bare TiO_2 measurement.

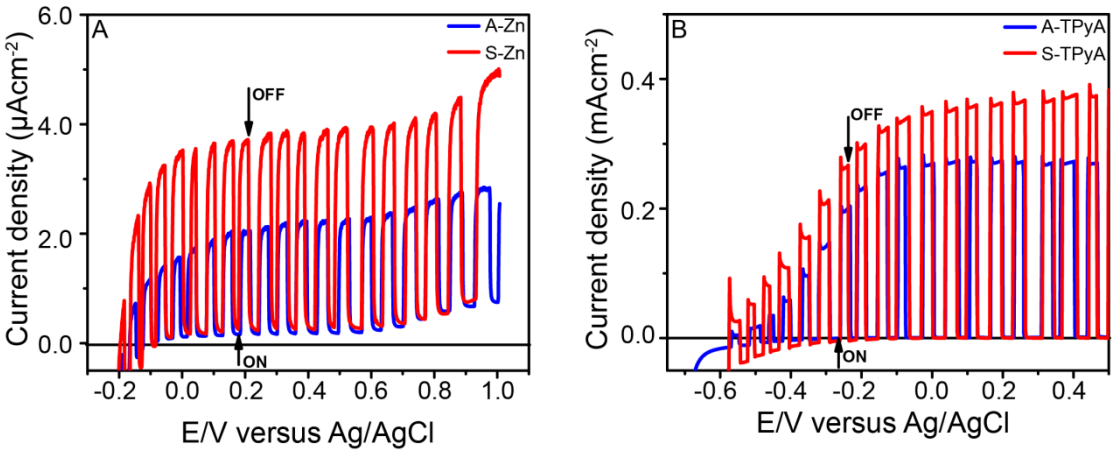

Figure S6: The current density as a function of the potential vs. the Ag/AgCl electrode, when the TiO_2 electrode is coated with self-assembled Zn-porphyrins (**A**) or with self-assembled TPyA (**B**) of either achiral (blue) or chiral (red) stacks. The measurements were performed at a scan rate of 10 mVs^{-1} by switching the light ON and OFF.

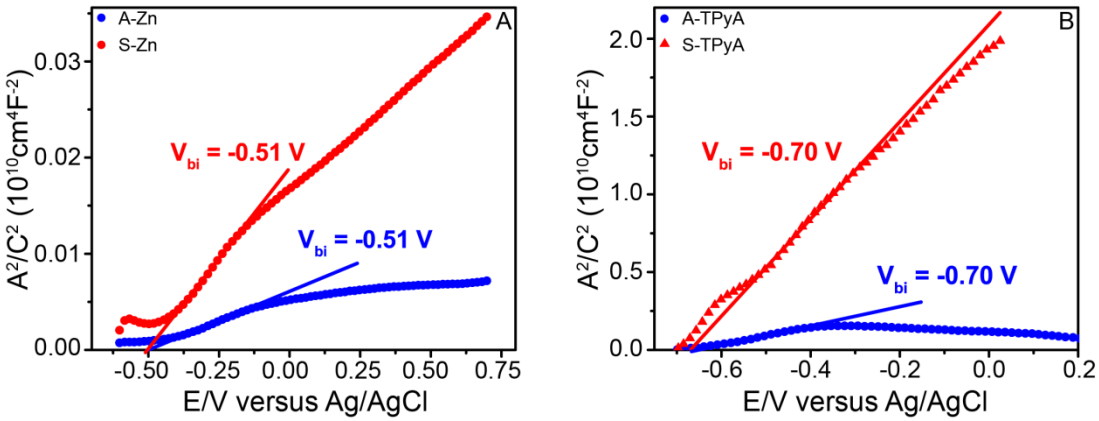

Figure S7: Mott-Schottky measurements obtained from a TiO_2 electrode coated with Zn-porphyrins (**A**) and TPyAs (**B**). Achiral analogues reported with blue symbols, chiral analogues with red symbols. The measurements were performed at a frequency of 1.99 kHz with an oscillation voltage of 20 mV, in the dark. The linear fits determine the flat band potential by the intercept with the E axis.

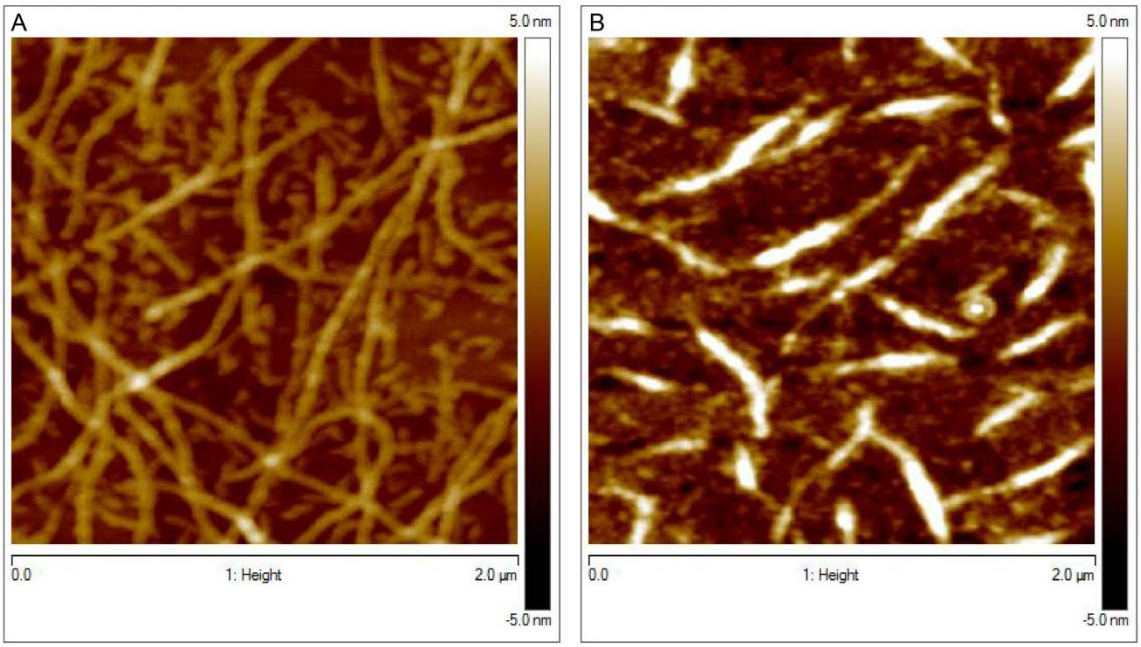

Figure S8: AFM images obtained from chiral (**A**) and achiral (**B**) Zn-porphyrins on HOPG

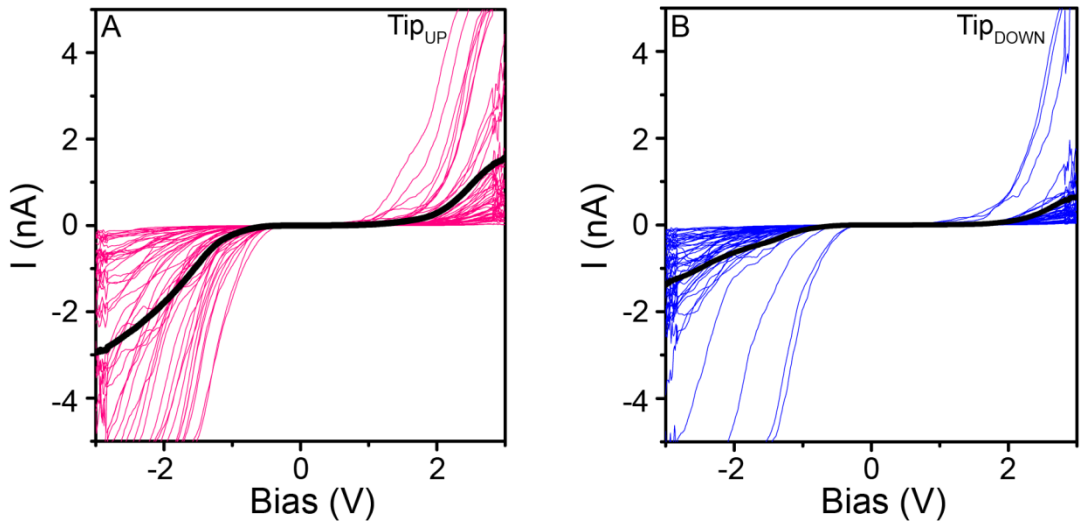

Figure S9: I-V curves obtained from chiral Zn-porphyrins using conductive probe AFM (color traces show individual measurements and the black trace shows the average).

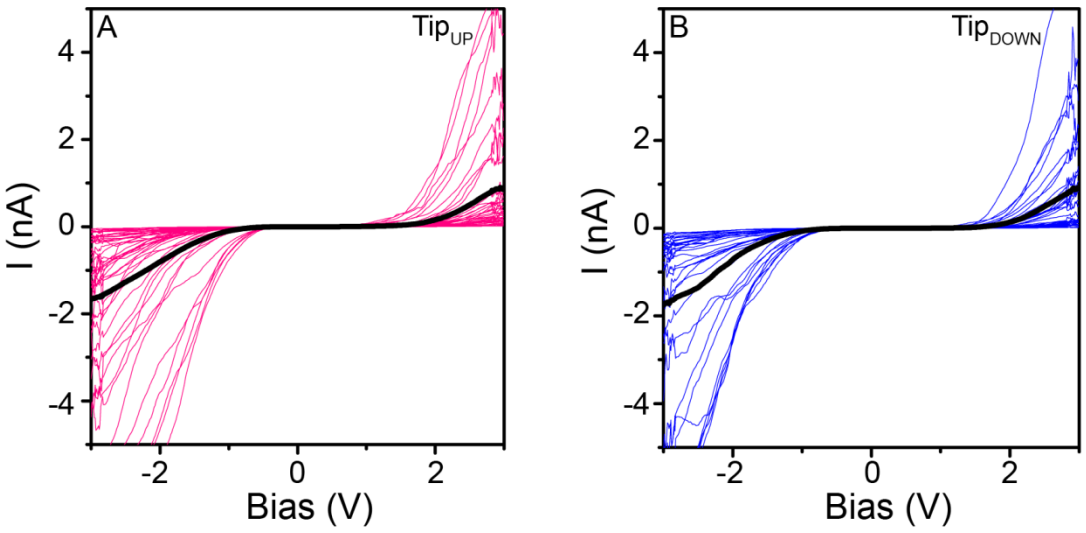

Figure S10: I-V curves obtained from achiral Zn-porphyrins using conductive probe AFM (color traces show individual measurements and the black trace shows the average).

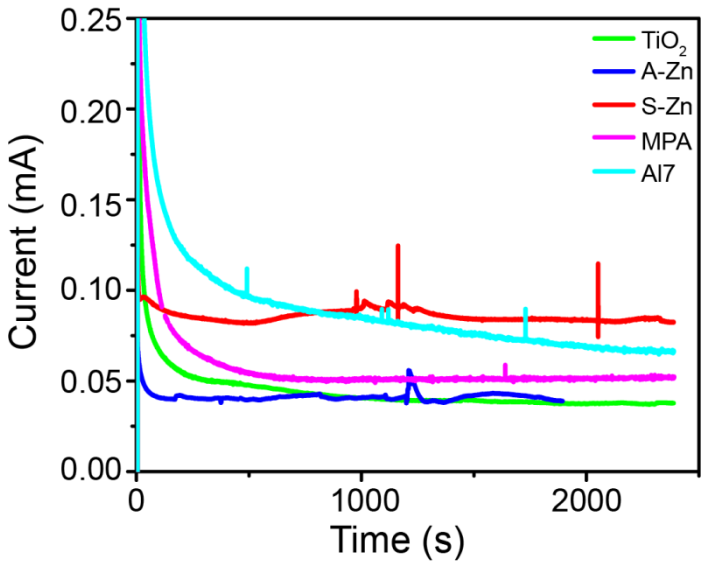

Figure S11: Current density as a function of time, on bare TiO_2 (green line) and when the TiO_2 electrode is coated with self-assembled Zn-porphyrins either achiral (blue line) or chiral (red line), MPA (magenta line) and Al7 (cyan line) to quantify the amount of hydrogen peroxide produced. The measurements were performed at 1.6 V versus Ag/AgCl.

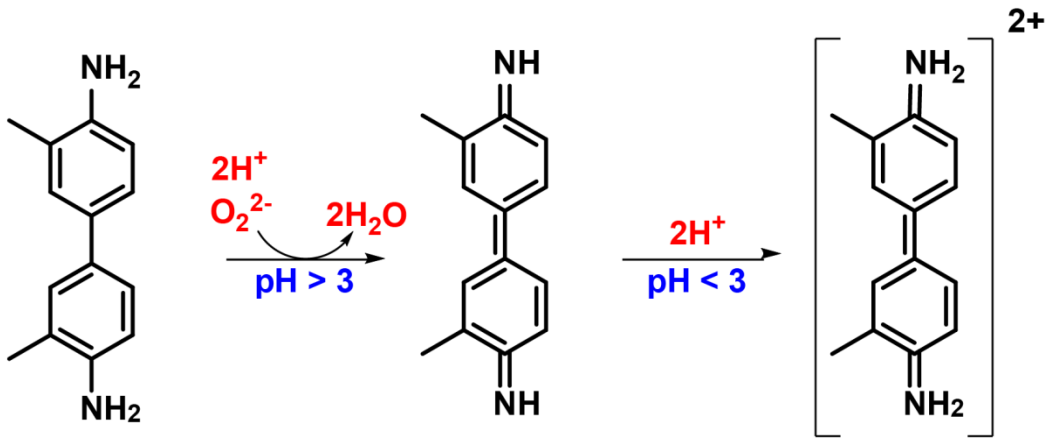

Figure S12: Reaction scheme between H_2O_2 and o-tolidine, spectrophotometric redox indicator.

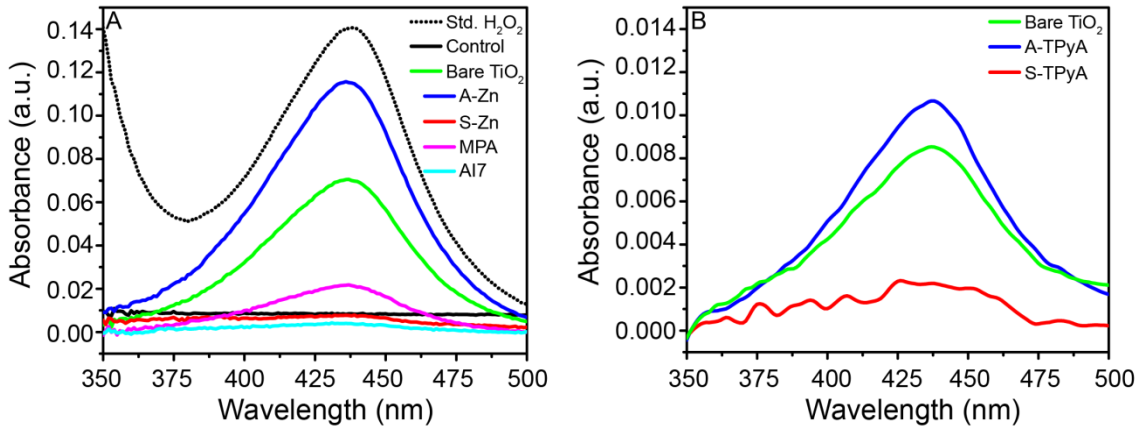

Figure S13: UV-vis absorption spectra from the titration with *o*-tolidine of the used electrolytes (0.1 M Na_2SO_4) after 40 min irradiation on functionalized TiO_2 electrodes with A-Zn, (**A**, blue line), *S*-Zn (**A**, red line), MPA (**A**, magenta line), Al7 (**A**, cyan line), A-TPyA (**B**, blue line), *S*-TPyA (**B**, red line), bare TiO_2 (green lines), The control refers to the titration of unused 0.1 M Na_2SO_4 with *o*-tolidine. The absorption using commercial H_2O_2 (**A**, dotted black line) is shown for reference.

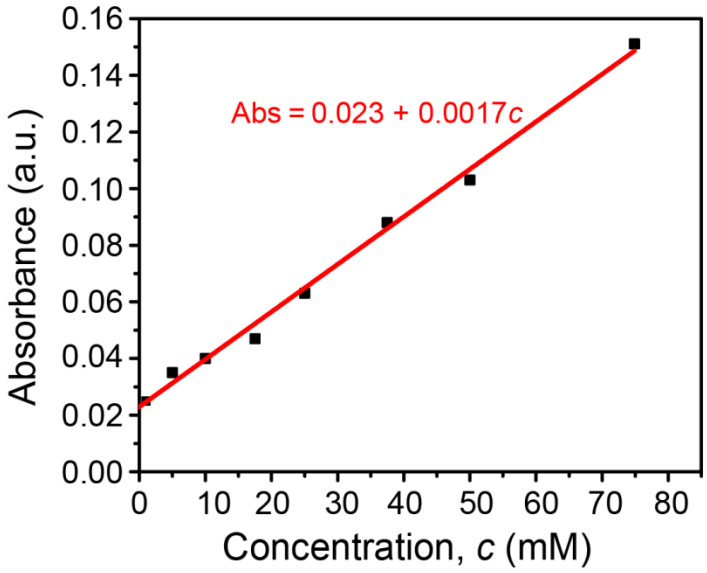

Figure S14: Calibration curve for the concentration of commercial hydrogen peroxide.

Table S1: Concentration of H_2O_2 calculated from the electrolyte solutions used in electrochemistry with TiO_2 coated with different molecules.

Molecule used to coat electrode	**H_2O_2 Concentration (m**molL^{-1}**)**
A-Zn	42.7 ± 5
Bare TiO_2	22.3 ± 4
MPA	2.7 ± 0.5
A-TPyA	-
S-TPyA	-----
S-Zn	-----
Al7	-----

References:

(1) Helmich, F.; Lee, C. C.; Nieuwenhuizen, M. M. L.; Gielen, J. C.; Christianen, P. C. M.; Larsen, A.; Fytas, G.; Leclère, P. E. L. G.; Schenning, A. P. H. J.; Meijer, E. W. *Angew. Chem. Int. Ed.* **2010**, *49*, 3939–3942.

(2) Helmich, F.; Lee, C. C.; Schenning, A. P. H. J.; Meijer, E. W. *J. Am. Chem. Soc.* **2010**, *132* (47), 16753–16755.

(3) Szelke, H.; Wadepohl, H.; Abu-youssef, M.; Krämer, R. **2009**, No. Scheme 1, 251–260.

(4) Adelizzi, B. Filot, A. W. Palmans, A. R. A.; Meijer, E. W. *Chem. - A Eur. J.* **2016**.

(5) Mtangi, W.; Kiran, V.; Fontanesi, C.; Naaman, R. *J. Phys. Chem. Lett.* **2015**, *6* (24), 4916–4922.

(6) Aragonès, A. C.; Aravena, D.; Cerdá, J. I.; Acís-Castillo, Z.; Li, H.; Real, J. A.; Sanz, F.; Hihath, J.; Ruiz, E.; Díez-Pérez, I. *Nano Lett.* **2016**, *16* (1), 218–226.

(7) Chakrabarti, S.; Pal, A. J. *Appl. Phys. Lett.* **2014**, *104* (1), 13305.

(8) Ellms, J. W.; Hauser, S. J. *J. Ind. Eng. Chem.* **1913**, *5* (11), 915–917.